Factors affecting the performance of a multi-tone carrier source based re-circulating frequency shifter*

Xi Li-Xia(席丽霞)†, Li Jian-Ping(李建平), Zhang Xiao-Guang(张晓光), Tian Feng(田 凤), and Zhang Wen-Bo(张文博)

State Key Laboratory of Information Photonics and Optical Communications, Beijing University of Posts and Telecommunications, Beijing 100876, *China*

(Received 15 February 2011; revised manuscript received 23 March 2011)

Generation of single-sideband (SSB) multi-carrier source based on a recirculating frequency shifter (RFS) is analysed theoretically and realized experimentally. The effects of affecting factors originating from the deviation from the right operation bias voltage and unbalanced amplitude, and the phase of the radio frequency (RF) drive signals on the performance of the multi-tone source are discussed in detail. Based on the theoretical analysis, high-quality 50-tone output is successfully realized. Experiments under some implementation imperfections are also carried out. The imperfect and low-quality output results are in good agreement with theoretical analysis.

Keywords: multi-tone carrier source, recirculating frequency shifter, affecting factors

PACS: 42.30.Lr, 42.79.–e, 42.81.–i **DOI:** 10.1088/1674-1056/20/8/084202

1. Introduction

In order to achieve the T-bit/s high-speed optical transmission required to meet the increasing demand for data traffic, coherent optical orthogonal-frequency-division-multiplexings (CO-OFDMs) with different modulation formats have been investigated widely in recent years.[1−13] In a CO-OFDM transmission system, a frequency-locked multi-carrier source is needed. There are various methods used to generate multi-carriers, including the typical cascaded Mach–Zehnder modulators (MZMs),[7] an optical frequency comb source based on a sine wave driven discrete mode (DM) laser,[8] and a single-side-band (SSB) modulator based on a recirculating frequency shifter (RFS).[2−6] Of the three technologies, the last one has the advantages of lower drive voltage and the ability to generate a larger number of carriers. In addition, these carriers are exactly frequency-locked. By applying this method, 24-tone[3−5] and 36-tone[2] multi-carrier sources have been generated successfully. Moreover, the crosstalk and stability of the multi-carrier generator under perfect operation conditions have also been investigated in Refs. [9] and [10]. In practice, there are many factors that influence multi-carrier output, such as an imbalance of the I/Q modulator (IQM) and radio-frequency (RF) drive signals.

In this paper, we theoretically and experimentally analyse the influence of affecting factors on the entire output of a SSB modulator-based RFS. These affecting factors include the deviation from the right bias voltage, the amplitude and the phase imbalance of RF drive signals. According to the theoretical analysis, a stable 50-tone carrier source with a flat spectrum and a high optical signal-to-noise ratio (OSNR) is demonstrated. The experimental results are in good agreement with the theoretical results.

2. Working principle of SSB modulator-based RFS

The schematic of the SSB modulator-based RFS is shown in Fig. 1(a). The configuration is a closed fibre loop, which consists of a 50:50 coupler, an IQM, an optical amplifier (OA), a tunable optical band-pass filter (OBF) and a polarization controller (PC). OA is used to compensate the modulation loss in the loop, OBF is used to control the number of desired carriers and PC is for realizing the states of polarization con-

*Project supported by the National Natural Science Foundation of China (Grant No. 60977049) and the Chinese Universities Scientific Fund (Grant No. BUPT 2009RC0413).

†Corresponding author. E-mail: xilixia@263.net and xilixia@gmail.com

© 2011 Chinese Physical Society and IOP Publishing Ltd

trol and stabilization of signals. The IQM is a core component in the loop. The structure of a commercially available IQM is illustrated in Fig. 1(b), which consists of two Mach–Zehnder modulators (MZMs) and a phase modulator (PM). $S_{\rm I}$, $S_{\rm Q}$ and $S_{\rm PM}$ are the electric signals operating on sub-MZM1, sub-MZM2 and PM, respectively. The tunable laser source (TLS) acts as a seed signal.

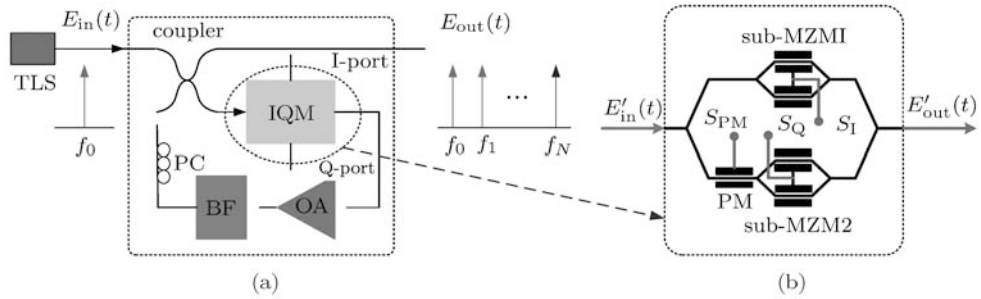


Fig. 1. Schematic diagram of (a) SSB modulator-based RFS and (b) the optical I/Q modulator.

The SSB modulator-based RFS working principle is as follows.

For a perfect IQM whose sub-MZMs operate in push-pull mode, the normalized transfer function can be written as

$$T = \frac{1}{2}\cos\left[\frac{\pi}{2V_{\pi\rm I}}(V_{\rm I}-V_{\rm bI})\right]\exp\left(-{\rm j}\,\frac{\pi V_{\rm bI}}{2V_{\pi\rm I}}\right) + \frac{1}{2}\exp\left(-{\rm j}\,\frac{\pi V_{\rm bPM}}{V_{\pi\rm PM}}\right)\cos\left[\frac{\pi}{2V_{\pi\rm Q}}(V_{\rm Q}-V_{\rm bQ})\right] \times \exp\left(-{\rm j}\,\frac{\pi V_{\rm bQ}}{2V_{\pi\rm Q}}\right), \quad (1)$$

where $V_{\pi\rm I}$, $V_{\pi\rm Q}$, and $V_{\pi\rm PM}$ are the half wavelength voltages of sub-MZM1, sub-MZM2 and PM, respectively; $V_{\rm bI}$, $V_{\rm bQ}$ and $V_{\rm bPM}$ are the DC bias voltages on sub-MZM1, sub-MZM2, and PM, respectively; $V_{\rm I}$ and $V_{\rm Q}$ are the driven RF signals. Corresponding to Fig. 1(b), $S_{\rm I} = V_{\rm bI} + V_{\rm I}$, $S_{\rm Q} = V_{\rm bQ} + V_{\rm Q}$, and $S_{\rm PM} = V_{\rm bPM}$.

If the IQM works under the ideal conditions, where $V_{\rm bI} = V_{\pi\rm I} = V_{\pi\rm Q} = V_{\rm bQ} = V_\pi$, $V_{\rm bPM} = V_{\pi\rm PM}/2$, $V_{\rm I} = V_{\rm PP}\cos(2\pi f_{\rm m}t)$, and $V_{\rm Q} = V_{\rm PP}\sin(2\pi f_{\rm m}t)$, the normalized transfer function of IQM can be simplified into

$$T_{\rm ideal} = \frac{1}{2}\{{\rm j}\sin[\delta_{\rm m}\cos(2\pi f_{\rm m}t)] + \sin[\delta_{\rm m}\sin(2\pi f_{\rm m}t)]\}, \quad (2)$$

where $\delta_{\rm m} = (\pi V_{\rm pp})/(2V_\pi)$ denotes the phase modulation depth.

Suppose that the input optical field is $E_{\rm in} = E_{\rm o}\exp({\rm j}\,2\pi f_0 t)$, where f_0 represents the seed frequency, the output electronic field after ideal IQM can be expressed as

$$E_{\rm out}(t) = \frac{E_{in}(t)}{2}\{{\rm j}\sin[\delta_{\rm m}\cos(2\pi f_{\rm m}t)] + \sin[\delta_{\rm m}\sin(2\pi f_{\rm m}t)]\}. \quad (3)$$

Using the Jacobi–Anger expansion and ignoring all the high order harmonics, the output of SSB-based RFS after the first round can be obtained as

$$E_1(t) = E_0{\rm J}_1(\delta_{\rm m})\exp[{\rm j}\,2\pi(f_0+f_{\rm m})t], \quad (4)$$

where ${\rm J}_1(\delta_{\rm m})$ is the first kind odd-order Bessel function. From Eq. (4) we can see that after the first round, the first frequency tone shift $f_1 = f_0 + f_{\rm m}$ is produced and the modulator drive voltage $V_{\rm pp}$ affects the output RFS. Then f_1 tone is split into two branches by coupler, one is put out and the other is coupled back to the input of the IQM. For the same reason, $f_2 = f_0 + 2f_{\rm m}$ tone shift will be generated in the second round. With endless recirculating in the loop, a series of frequency tones, $f_3 = f_0 + 3f_{\rm m}$, ..., $f_{\rm N} = f_0 + Nf_{\rm m}$, ... will be produced. By adjusting the central wavelength and bandwidth of the bandpass filter placed in the loop, we can obtain N tone multi-carriers we wanted and filter out those frequency tones beyond bandwidth.

In fact, high order harmonics will be produced in the modulation process, which will affect the performance of the RFS output. We have studied the crosstalk factor in Ref. [10]. Beside the crosstalk, which has also been investigated in Refs. [9] and [10], the deviations of bias operation voltage and the imbalance of RF clock drive signal in the actual operation

also seriously affect the performance of the RFS output. We will discuss them in the following.

3. Theoretical analysis of affecting factors

Firstly, we analyse the influence due to the deviation of the bias voltage. Assume that the IQM is perfectly balanced and that the RF drive signals are balanced, which are corresponding to the case $V_{\pi\mathrm{I}} = V_{\pi\mathrm{Q}} = V_\pi$, $V_\mathrm{I} = V_\mathrm{PP}\cos(2\pi f_\mathrm{m}t)$, and $V_\mathrm{Q} = V_\mathrm{PP}\sin(2\pi f_\mathrm{m}t)$. Suppose that the deviation of DC bias voltages from the right bias operation points are ΔV_bI, ΔV_bQ, and ΔV_bPM, respectively. Then equation (1) can be expressed as

$$\begin{aligned} T = {} & \frac{\mathrm{j}}{2}\sin\left[\delta_\mathrm{m}\cos(2\pi f_\mathrm{m}t) + \delta_\mathrm{bI}\right]\exp(\mathrm{j}\,\delta_\mathrm{bI}) \\ & + \frac{1}{2}\sin\left[\delta_\mathrm{m}\sin(2\pi f_\mathrm{m}t) + \delta_\mathrm{bQ}\right] \\ & \times \exp\left[\mathrm{j}\,(\delta_\mathrm{bQ} - \delta_\mathrm{bPM})\right], \end{aligned} \tag{5}$$

where

$$\Delta\delta_\mathrm{bI} = (\pi\Delta V_\mathrm{bI})/(2V_{\pi\mathrm{I}}), \quad \Delta\delta_\mathrm{bQ} = (\pi\Delta V_\mathrm{bQ})/(2V_{\pi\mathrm{Q}}),$$

and $\Delta\delta_\mathrm{bPM} = (\pi\Delta V_\mathrm{bPM})/(V_{\pi\mathrm{PM}})$ represent the bias voltage deviations from the right operation voltage respectively.

In order to observe the influence of the deviation of the bias voltage on the output, we simulate different cases for the first round output according to Eq. (5). The results are given in Fig. 2, showing that more harmonics appear when the bias voltages are deviated from the ideal points. More harmonics will result in serious crosstalk. Obviously, to reduce the harmonics crosstalk, we should take the bias voltages that are closest to the right operation voltages as much as possible in practice.

Secondly, the effect of the imbalance of RF drive signals on the RFS output is analysed. For this case, we focus on the effects of the voltage amplitude and phase difference between I-port and Q-port RF drive signals on the output. Assume that the IQM is perfectly balanced and all modulators operate at their right points, namely, only the phase deviation $\Delta\theta$ and voltage amplitude difference ΔV_m between the two RF signals are considered. In this case, the transfer function of the IQM can be expressed as

$$\begin{aligned} T = {} & \frac{\mathrm{j}}{2}\sin\left[\delta_\mathrm{m}\cos(2\pi f_\mathrm{m}t)\right] \\ & + \frac{1}{2}\sin\left[(\delta_\mathrm{m} + \Delta\delta_\mathrm{m})\sin(2\pi f_\mathrm{m}t + \Delta\theta)\right], \end{aligned} \tag{6}$$

where $\Delta\delta_\mathrm{m} = (\pi\Delta V_\mathrm{m})/(2V_\pi)$.

We also simulate the first round output or transfer function output for different cases according Eq. (6). In the simulation process, we use the power difference ΔP_m instead of the voltage amplitude difference ΔV_m. The simulated results are shown in Fig. 3. We can see that there is no even-order harmonics crosstalk even though the RF drive signals are unbalanced. These results are different from the above situations. Moreover, $\pi/4$ phase deviation will result in more serious signal degradation, which is concluded from Fig. 3 where the power of crosstalk component f-1 in case (b) is larger than that in case (a). In practice, we should adjust the amplitudes of the two RF signals to be equal and phase deviation to near zero.

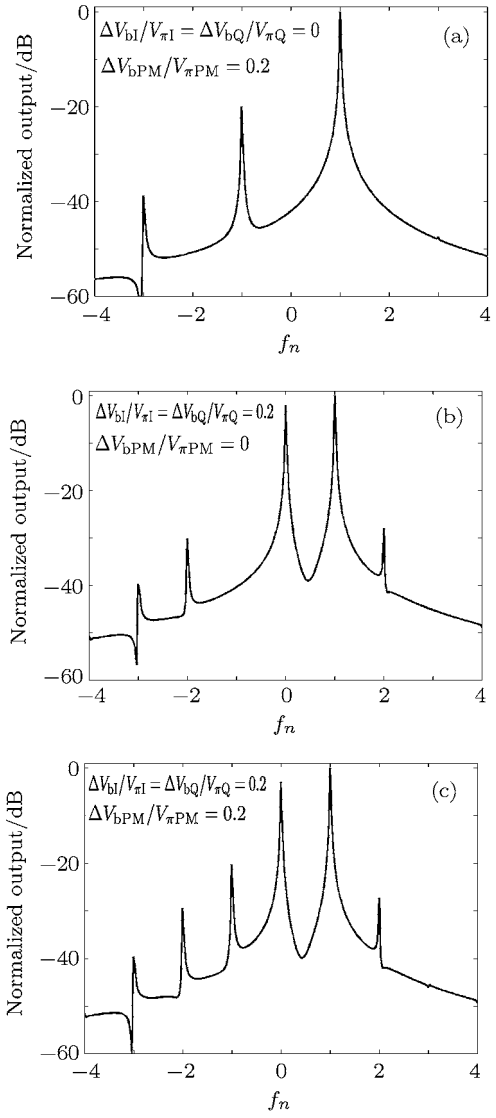


Fig. 2. Effects of bias voltage deviation on the first round output in different cases.

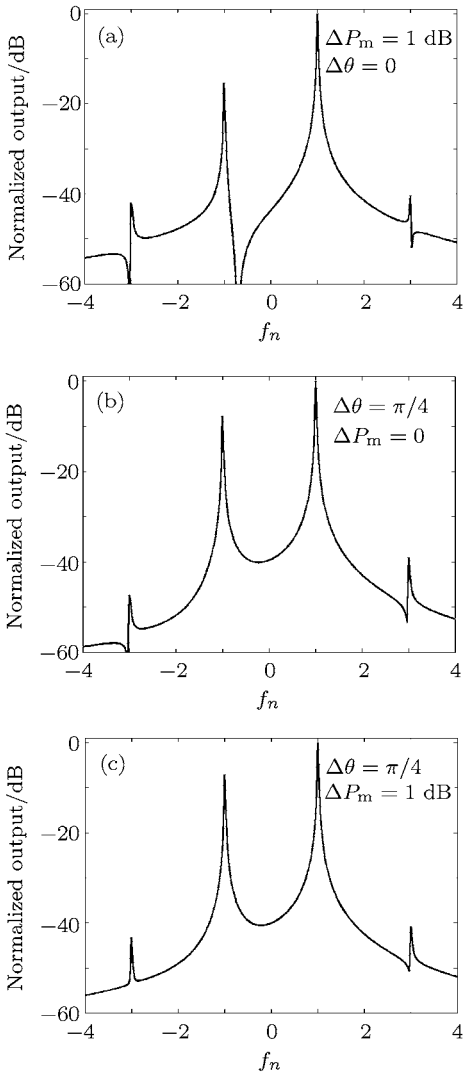


Fig. 3. Effects of amplitude and phase imbalance of RF drive signals on the first round output in different cases.

4. Experimental demonstration

We study the influence of the affecting factors on the multi-carrier output in experiment. The experimental setup is shown in Fig. 1(a). The TLS wavelength is $\lambda_0 = 1549.9$ nm ($f_0 = 193.425$ THz) and the bandwidth of optical band-pass filter is set to be 5 nm. The clock signals with the frequency 12.5 GHz are obtained from the signal generator, two microwave power amplifiers and two adjustable power attenuators are used to adjust the driven RF signals input power. The phase difference is obtained by adjusting the time delay of the signal generator.

First, we adjust the parameters to the ideal values. The best output for the transfer function is obtained and, as shown in Fig. 4(a), there are no other harmonics except for the desired f_1. The flat and stable 50-tone multi-carrier output with a spacing of 12.5 GHz is successfully achieved, which is shown in Fig. 4(b).

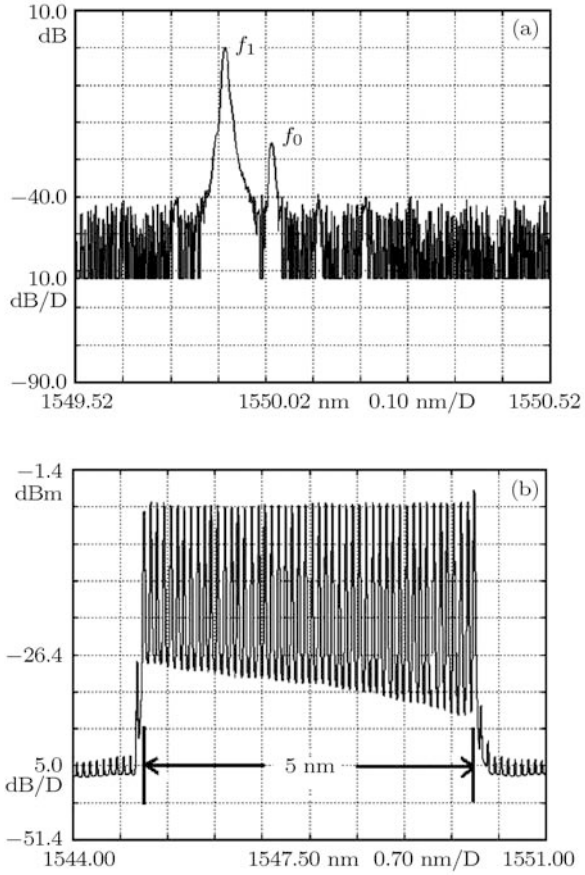


Fig. 4. Experimental results under the balanced operation condition, showing (a) transfer function output and (b) 50-tone output.

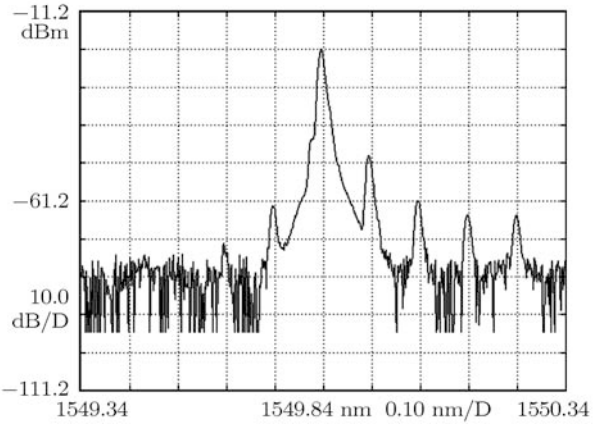


Fig. 5. Optical spectrum of the transfer function with high-order harmonics

In order to investigate the influence of the affecting factors on the performance of the multi-carriers output in detail, we break down the balanced parameters. Figure 5 shows the transfer function output

for the case where the bias voltages and the RF signals are all unbalanced. We can see that there are many other harmonics that seriously affect the performance of the output. Subsequently, we discuss the effects of bias voltage deviation and RF signal imbalance, respectively. Adjust the bias voltage to be away from the right operation point, the distorted outputs of the multi-carrier source are obtained as shown in Fig. 6, in which the parameters are $\Delta V_{\rm bI} = 0.7$ V,

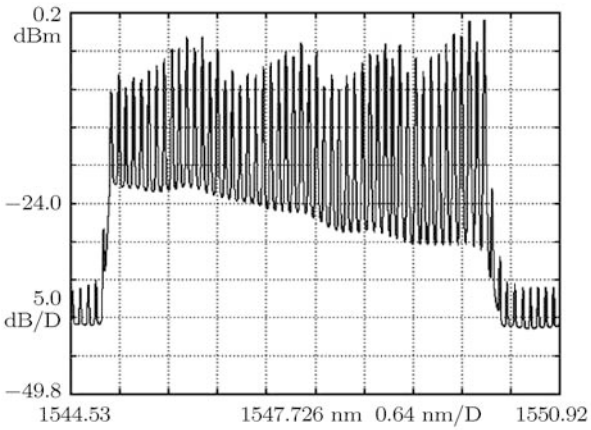


Fig. 6. Output spectrum with $\Delta V_{\rm bI} = 0.7$ V, $\Delta V_{\rm bQ} = \Delta V_{\rm bPM} = 0$.

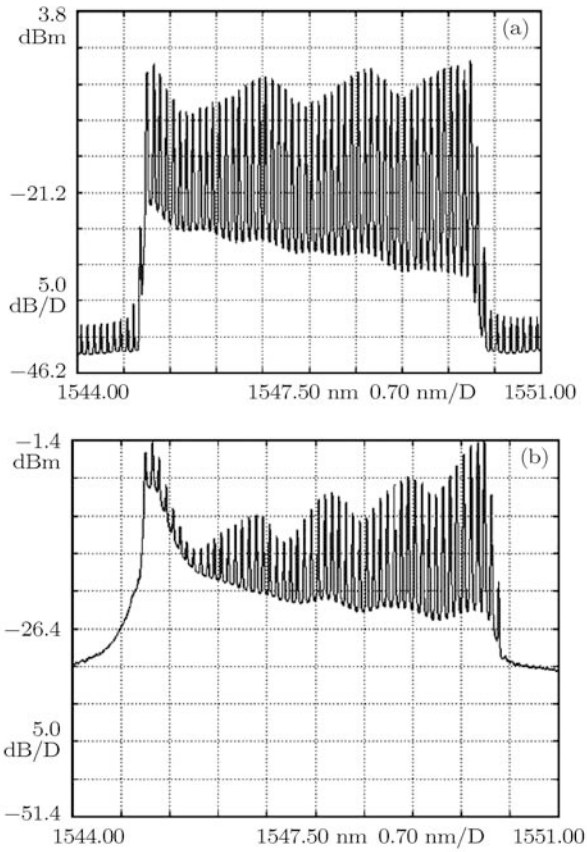


Fig. 7. Output spectra with (a) $\Delta P_{\rm m} = 1$ dB and $\Delta\theta = 0$ and (b) $\Delta P_{\rm m} = 0$ dB, $\Delta\theta = \pi/4$.

$\Delta V_{\rm bQ} = \Delta V_{\rm bPM} = 0$. Adjust the RF power attenuators to make the driven RF signals between the two sub-MZMs have a power difference of 1 dB. The output spectrum (Fig. 7(a)) shows that the quality of the output signal becomes worse. If the time delay of the signal regenerator is adjusted, the phase difference between the two RF signals will change. Figure 7(b) shows the output spectrum when the phase deviation from right value is $\pi/4$. The results are much worse than the results shown in Fig. 7(a), which is coincident with the above theoretical analysis.

To achieve a high-quality multi-carrier source-based RFS, some other factors should be taken into account, such as the external cavity laser (ECL) source with more stable frequency and phase, optical amplifier with lower noise figure (NF) and IQM with lower insertion loss, besides the above implementation imperfections.

5. Conclusion

Guided by the theoretical analysis, a stable and high-quality 50-tone multi-carrier was successfully achieved experimentally. The effect of the crosstalk component induced both by the deviation of DC bias voltage from the right operation point and by the imbalance of the amplitude and phase of the RF drive signals on the output of SSB-based RFS multi-carrier generator has been analysed theoretically and experimentally. The theoretical and the experimental results may provide a useful guidance for achieving the high-quality SSB-based RFS multi-carrier source for Tb/s multi-carrier transmission in practice.

References

[1] Liu X, Gill C, Chandrasekhar S, Buhl L, Earnshaw M, Cappuzzo M, L Gomez L, Chen Y, Klemens F, Burrows E, Chen Y and Tkach R 2010 *IEEE Photonics Journal* **2** 330

[2] Ma Y, Yang Q, Tang Y, Chen S and Shieh W 2009 *Opt. Express* **17** 9421

[3] Chandrasekhar S, Liu X, Zhu B and Peckham D 2009 *European Conference on Optical Communication* (ECOC), September 20–24, 2009, Vienna, Austria, post-deadline paper PD2.6

[4] Zhu B, Liu X, Chandrasekhar S and Peckham Jr D R 2010 *IEEE Photon. Technol.* **22** 826

[5] Liu X, Chandrasekhar S, Zhu B and Peckham D 2010 *Proc. Optical Fibre Commun.* (OFC), March 22–26, 2010, San Diego, CA, 2010, paper OWO2

[6] Chen S, Ma Y and Shieh W 2010 *Proc. Optical Fibre Commun.* (OFC), March 22–26, 2010, San Diego, CA, 2010, paper OMS2

[7] Healy T, Gunning E, Ellis A and Bull J 2007 *Opt. Express* **15** 2981

[8] Maher R, Anandarajah P, Ibrahim S, Barry L, Ellis A, Perry P, Phelan R, Kelly B and Gorman J 2010 *European Conference on Optical Communication* (ECOC), September 19–23, 2010, Torino, Italy, paper P3.07

[9] Ma Y, Yang Q, Tang Y, Chen S and Shieh W 2010 *J. Lightw. Technol.* **28** 308

[10] Li J P, Li X, Zhang X G, Tian F and Xi L X 2010 *Opt. Express* **18** 17597

[11] Tan Z Y, Guo X G, Cao J C, Li H and Han Y J 2010 *Acta Phys. Sin.* **59** 2391 (in Chinese)

[12] Xin X J, Ma J X, Zhang Q, Deng C G, Wang K R, Yu C X and Liu B 2009 *Chin. Phys.* B **18** 3449

[13] Chen H T, Jia X H, Wang F and Zhong D Z 2007 *Acta Phys. Sin.* **56** 2637 (in Chinese)